JPhys Energy

PERSPECTIVE • OPEN ACCESS

MXenes and the progress of Li–S battery development—a perspective

To cite this article: Juan Balach and Lars Giebeler 2021 *J. Phys. Energy* **3** 021002

IOP Publishing J. Phys. Energy 3 (2021) 021002 https://doi.org/10.1088/2515-7655/abd5c4

Journal of Physics: Energy

OPEN ACCESS

PUBLISHED
1 March 2021

PERSPECTIVE

MXenes and the progress of Li–S battery development—a perspective

Juan Balach[1] and **Lars Giebeler**[2]

[1] Research Institute for Energy Technologies and Advanced Materials (IITEMA), National University of Rio Cuarto (UNRC)-National Council of Scientific and Technical Research (CONICET), National Route No. 36, Km 601, Río Cuarto 5800, Argentina
[2] Leibniz Institute for Solid State and Materials Research (IFW) Dresden e.V., Helmholtzstr. 20, 01069 Dresden, Germany

E-mail: jbalach@exa.unrc.edu.ar **and** l.giebeler@ifw-dresden.de

Keywords: MXene phase, 2D material, lithium–sulfur battery, rational design, self-healing electrode, device minimization, self-charging

Supplementary material for this article is available online

Abstract

Lithium–sulfur (Li–S) battery has attracted tremendous interest owing to its high energy density at affordable costs. However, the irreversible active material loss and subsequent capacity fading caused by the uncontrollable shuttling of polysulfides have greatly hampered its commercial viability. MXenes, a novel class of 2D materials derived from nano-layered MAX phases, have been shown the potential to push the development of sulfur-based batteries to a next level owing to their high conductivity, strong polysulfide affinity and electrocatalytic properties. This perspective article focuses on the possible implications that MXene-based materials will have in the development of advanced sulfur-based batteries and their potential application in different upcoming technologies. In four sections possible developments are outlined which can be reached in the next 10 years, that enable a highly reliable, minimized Li–S battery finally combined with energy harvesters to fabricate autonomous power supplies for the next generation of microscaled devices like meteorological or geotechnical probes, wearable (medical) sensors or other suitable mobile devices. Finally, a flowchart illustrates the possible way to realize some important milestones for the certain possible steps with significant contributions of MXenes.

1. Introduction

The first reports on single-layer graphene in 2004 and 2007 have motivated the research community to explore other 2D materials with prospective novel and interesting properties [1, 2]. Not 10 years later another class of 2D materials has been reported in 2011 [3] and has quickly raised large attention: MXenes. The name 'MXene' emphasizes the affinity with the inherited chemical features of the MAX phases and the morphological similarity with graphene. MAX phases, denoted by the general formula $M_{n+1}AX_n$, are the precursor to prepare MXenes, where M is a transition metal mainly of group IVb, Vb or VIb, A represents main group elements of the groups IIIa, IVa and Va and X is related to carbon and/or nitrogen. These compounds belong to the large family of transition metal carbides, carbonitrides or nitrides and hand several properties down to the MXenes, like an almost metallic electrical conductivity or the mechanical stability.

To prepare a MXene, the A layer of the corresponding MAX phase is etched leaving the M and X layers almost untouched but generate surface functional terminating groups like O, OH, Cl and/or F, abbreviated by T, to rewrite the general formula of a MAX phase to that one of a MXene with $M_{n+1}X_nT_x$ [4].

Such different possible chemical compositions and terminating functional groups induce multiple interesting physical and chemical properties [5–9]. Therefore, MXenes hold great promise to be applied for an umbrella of applications, such as energy storage and conversion [4, 9–19], for (photo)catalysts [10–12],

sensors [10, 12, 20, 21], in electronics [13, 22–24], electromagnetics [9, 10, 25, 26], optics [10, 20, 24, 27–33], for (bio)medicine [9, 10, 19, 20, 34–37], environmental aspects [11, 38–70] and many more [4, 10–12, 41–44].

According to the unique properties of MXenes, they have raised high hopes to solve issues that are actually tricky to handle with usual solutions. These promising possibilities also comprehend electrochemical energy storage systems. After showing significant results for ion intercalation batteries and (super)capacitors [10, 11, 16, 18, 44–47], MXenes are supposed to become a novel electrode material or, at least, a part of the electrode composite. Beside all positive aspects, it is noted that negative properties may need to be taken into account like instability against air, quick change of the metallic conductivity to semiconducting depending on the multiple of *n* and the terminating group or the etching process, if hydrofluoric acid or fluorine-containing compounds are used. These issues need to be checked before the utilization of MXenes. Nevertheless, many positive examples have been found where MXenes and MXene-based materials or composites have been successfully applied [11, 39, 48].

The step to benefit from the advantageous properties was quite small and quickly spread to sulfur batteries as well. In a first publication of Liang *et al* [49], the MXene Ti_2CT_x was used as sulfur host substrate as it can by-pass the isolating properties of sulfur with the almost metallic conductivity. Additionally, polysulfide-retaining coordination and mechanical flexibility to compensate the volume changes during cycling are other positive features of MXenes. With different preparation techniques, sulfur was transferred into the host and during the electrochemical test the suitability and the chemical stability of the S/Ti_2CT_x cathode vs Li/Li^+ were proven. After that initial work, more MXenes have been functionalized to become valuable sulfur hosts [50]. Later, MXenes have been introduced to functionalized separators as well [46, 51, 52]. From that point on, it was clear that the sulfur battery chemistry can significantly benefit from MXenes.

As insinuated in the previous section, this perspective article focuses on room temperature lithium–sulfur (Li–S) batteries with improvements related to the properties of MXenes. Together with already existing literature, the extension of the application to the microscale and a later coupling with energy harvesting systems to enable autonomous power sources is theoretically developed. The Li–S battery is treated as the next-generation energy storage system due to the high specific capacity of 1672 mAh g^{-1} for sulfur in the cathode, the high theoretical specific energy of 2600 Wh kg^{-1} and the high energy density of 2800 Wh l^{-1}, that are almost five-fold larger than for typical lithium-ion (Li-ion) batteries [5, 45]. Additionally, the sulfur system reacts with lithium according to a conversion mechanism implying faster charging and discharging compared to conventional Li-ion batteries. Beside the interesting electrochemical properties, another main advantage to use sulfur in such batteries is the high natural abundance and therewith a possible favorable price of the final product. Hence, it seems reachable to avoid rare elements and enables the related industry to save valuable resources.

Recent developments of the sulfur battery have reached a high standard and the Li–S system is discussed to be commercialized. Oxis Energy, Sion Power and other companies try to introduce and establish Li–S cells in the market but these plans and campaigns mainly cover large format pouch cells, synonymically known as coffee bag cells, designated for automative traction or grid support storage.

What has not yet been paid large attention to is the miniaturization of Li–S batteries and their possible coupling with energy harvesting devices. This relation can be explained by the still challenging chemistry between electrodes and electrolyte that is often focused on the ubiquitous shuttle effect. This term describes the formation of polysulfides during the redox processes which migrate through the cell to deplete the cathode on sulfur or poison the anode. Another issue is found in the relatively high amount of electrolyte per gram of sulfur which is necessary to sufficiently operate this secondary cell type. To play off the advantages of Li–S against Li-ion intercalation batteries, high volumetric energy densities must be reached which is enabled by low electrolyte volumes or by a solid state-related approach.

To inhibit the shuttle effect and decrease the electrolyte volume but also to meet additional requirements like high reliability, MXenes show the potential to push such developments of sulfur-based batteries. With the structure variability, e.g. in elements and terminal groups, and the ability to tailor the properties of MXenes, it seems to be a reasonable step to intensify the utilization in Li–S batteries, as motivated and recommended in a recently published review [53]. On the way to become a highly reliable MXene-based electrode, the addition of a binder polymer with so-called self-healing properties can offer the necessary advantage. Such polymer can fix the electrode material in a matrix-like environment. The self-healing typically acts via the reformation of previously broken bonds, e.g. after mechanical fracture of the electrode composite during charging and discharging [54, 55]. With this concept, the stability of the electrode is enhanced and performance and life time may increase significantly.

After successful improvement to a reliable MXene-based electrode the miniaturization step of the Li–S battery can be started. The promises of the electrical storage ability of Li–S batteries should be brought to

small dimensions as the applications for miniaturized devices, like for human-body probing, medication or other wearable products with many potential functionalities for almost every situation rapidly grows. Along with such developments, device combinations and number of tasks to fulfill, complex operation and computation scenarios can be reached. Additionally, long durations are highly preferred. These situations make high-performing and high-energy powering units necessary and the Li–S system is in principle able to provide both. As high power consumption quickly discharge the battery system, an integration of an energy harvesting device can be needful. Different harvesting systems can make use of several energy sources and are able to convert this energy into electrical power to (re)charge the battery. Coupling the energy harvesting device together with the battery for energy storage, self-charging is possible without mains connections. Here, the respective sensor or other application can be used highly independent. Such a combined system can act as an autonomous power supply and is therefore qualified for the field application, not only in wearable (medical) sensors but for rough or extreme conditions in meteorological or geological and geotechnical probes or for monitoring volcanos and seismic activities.

To realize this ambitious development, a flowchart proposes several (rough) steps starting from the rational design approach for building a better battery via the minimization strategy and the engineering to highly reliable materials with self-healing properties to finally reach the goal of an autonomous (micro)power supply after integrating an electrical energy harvesting device used as a power source for grid-independemt self-charging of a Li–S microbattery. From the given ideas supported by existing literature, other sulfur batteries, even in the solid state type, may benefit from the potential progresses as well.

2. Just building a better battery: with rational design of MXenes to their beneficial application in Li–S batteries

To reach the final goal of an autonomous power supply, a rational design strategy can be taken as a possible starting point. It can help to adapt the material to reach a specific property that significantly supports the designated application. This strategy comprises typical experimental planning and even makes use of high-throughput screening facilities. With increasing computing power, the same strategy can be configured from virtual developments that predict properties in computational studies. A future trend may include both ways as not all complex properties will available from theoretical explanations and not all experimental results will be understood without computational methods. Numerous examples are found crossing many disciplines in pharmacology and medicine [56–59], in material science for polymers [60], alloys and intermetallics [61, 62] to engineer optical and magnetic properties in physics [61, 63] or in chemistry for metal-organic [64, 65] or covalent-organic frameworks [66], zeolites and other porous inorganic compounds [67–69] or catalysts [70–73]. These examples are aimed to tune the material properties and to explain underlying mechanisms. With this knowledge, it is possible to directly intervene at negatively affecting stages and offer solutions to by-pass critical issues. Additionally, rational design approaches can save time and resources, at least monetary, depending on the possible influence of the measure and the complexity of the treated system.

For batteries, rational design approaches have been experimentally realized for cation-related intercalation on the positive electrode, e.g. optimizing transport properties [74], pore engineering [75] and lattice spacing for the respective cation [76, 77], or for alloying systems for the negative electrode to improve their storage properties to high capacities [78]. Following a similar rational design strategy concept, theoretical calculations have been performed in order to study and understand the chemical interaction of MXene materials with Li_2S and polysulfide intermediates. From these results, a guideline for the rational choice of MXene-based sulfur host matrices or separator coatings are provided to further optimize the electrochemical performance and cycle life of the Li–S battery system.

2.1. Experimentally driven rational design

Since the emergence of graphene nanosheets in 2004 [1], 2D materials have gained great attention in the field of energy storage, in addition to many other applications. In general, 2D materials offer multiple physicochemical features which are advantageous for electrode material applications: (a) they possess inherent high surface-to-volume ratios, (b) they are conductive for electron transport, (c) their exposed edges and some irregularities on the basal planes are propitious for chemical modification and, (d) they are suitable for fabricating flexible electrodes due to their good mechanical stability [79, 80]. However, the diffusion of electrolyte ions through 2D layered materials could be limited by the narrow interlayer spacing. Further, the forced intercalation of ions under a potential gradient could deteriorate the structural stability of these materials upon cell operation. These issues affect the electron and ion diffusion kinetics in the electrode and the electrochemical reversibility of the cell. Therefore, the control over interlayer spacing and the

restacking of nanosheets are crucial aspects, to which attention should be paid to, during the realization of an enhanced electrochemical performance [76, 77, 81].

In 2015, a 2D-layered MXene was introduced in Li–S batteries by the Nazar group, attracting particular interest owing to their inherent high conductivity, chemical stability, mechanical robustness and self-functionalized surface [49, 82, 83]. Interestingly, the etching and exfoliation processes involved in the production of MXenes directly create a (multi)layered functional material with a surface termination-mediated interlayer spacing. This interlayer spacing serves as a planar channel system for efficient electrolyte ion diffusion. Additionally, it provides active sites for anchoring sulfur-based species. Experimental results revealed that the active material interacts with the MXene surface by the chemisorption of sulfur-based species on 'acidic' Ti sites and hydroxyl surface groups, thus promoting the electron transport and the polysulfide conversion kinetics [49]. The terminations on the chemically active surface of MXenes will consequently play a pivotal role in the interaction with soluble polysulfides and, hence, in the polysulfide shuttle control.

Initially, due to the metallic conductivity and surface chemistry of MXenes, binary sulfur-$Ti_3C_2T_x$ MXene composites were proposed as the positive electrode for Li–S batteries [49, 52]. However, the restacking of the delaminated $Ti_3C_2T_x$ MXene material still persists after exfoliation via van der Waals interactions among $Ti_3C_2T_x$ layers, thus limiting both the impregnation of molten sulfur to the whole scaffold during composite preparation and the diffusion of ions during cell operation. To circumvent this hurdle, 3D MXene-based architectures have been rationally designed by incorporating a nanomaterial which acts as a spacer to prevent the self-stacking of the MXene nanosheets (figure 1(a)). Interestingly, the introduced nanospacer could also serve as a redox mediator to further enhance the polysulfide affinity and promotes the redox solid–liquid/liquid–solid phase transformation of the active material by either an improved conductivity or electrocatalytic effects [84–87]. To this end, graphene [88–90], reduced graphene oxide [91], carbon nanotubes (CNTs) [92, 93], carbon compounds [94, 95], metal oxides [96–98], metal sulfides [99], functional polymers [100] and even $Ti_3C_2T_x$ nanodots [101] have been chosen. These approaches generate 3D-like complexes that slightly expand the MXene interlayer spacings and provide a highly accessibe pathway for fast charge/ionic transport through the entire cathode architecture. For instances, the growth of $Ti_3C_2T_x$ nanodots on the surface of $Ti_3C_2T_x$ nanosheets not only acted as an effective spacer to guard the $Ti_3C_2T_x$ nanosheets from restacking but also improved the polysulfide adsorption capability owing to the highly polarized active sites of the nanodots (figures 1(a) and (b)) [101]. Furthermore, the close contact of the $Ti_3C_2T_x$ nanodots with the $Ti_3C_2T_x$ nanosheet surface reduces theinterfacial resistance and promote the polysulfide redox kinetics. Consequently, the designed $Ti_3C_2T_x$ nanodots-$Ti_3C_2T_x$ nanosheets/S cathode with a very high sulfur loading of 13.8 mg cm^{-2} demonstrated high specific, areal and volumetric capacities of 1000 mAh g^{-1}, 13.7 mAh cm^{-2} and 1957 mAh cm^{-3}, respectively (figure 1(c)). It is worth mentioning that, as MXenes offer some similarities to carbons, the doping of the MXene structure, e.g. with nitrogen, could also improve both cyclability and polysulfide retention properties [95]. Since the intriguing feature of MXenes have ignited extensive research enthusiasm, many examples of MXenes and MXene composite materials have been proposed for improving the performance of Li–S cells. Table S1 (supporting information) (available online at stacks.iop.org/JPENERGY/3/021002/mmedia) summarizes the research progresses on MXene-based sulfur host materials and MXene-based functional separator coatings for Li–S batteries.

2.2. Approaches for rational design with computational methods

The fundamental understanding of chemical reaction mechanisms in new complex materials, e.g. MXenes, can become an intricate and laborious process if only experimental information are accessible. Here, the use of theoretical calculations appears as the most accurate solution to elucidate and understand the interaction of MXene materials and sulfur-derived species at the atomic scale, and even more suitable, to predict properties of materials not yet synthesized [103–105]. In an attempt to provide a guideline to the rational choice of MXene-based sulfur hosts, first-principles calculations based on the density functional theory (DFT) method were performed. The MXene substrates as the systems of study have been selected from a broad variety: M_2CT_2, $M_3C_2T_2$ and M_2NT_2 (M = Ti, V, Cr, Nb, Hf and Zr; T = N, S, O, P, F, and Cl) [102, 106–114]. In general, similar benefits have been highlighted for MXene materials, such as their strong affinity toward polysulfide intermediates and their metallic features which facilitate the electrochemical activity during cell operation. Calculations on the binding affinity revealed, that functionalized Ti_2C-based MXenes could form Ti–S bonds with sulfur-based species via Lewis acid-base interactions, since Ti atoms with unoccupied orbitals could accommodate a pair of electrons from the sulfur atoms [102, 106–109]. Interestingly, Ti_2C-based MXenes with surface vacancy sites can form new and strong Ti–S bond terminations upon contact with sulfur or polysulfides, generating a S-functionalized MXene. The resulting Ti_2CS_2 MXene notably possesses stronger binding affinity for lithium (poly)sulfides than Ti_2CO_2 and Ti_2CF_2 MXenes related to higher binding energies (figure 1(d)) [102]. Further studies on O-functionalized MXenes

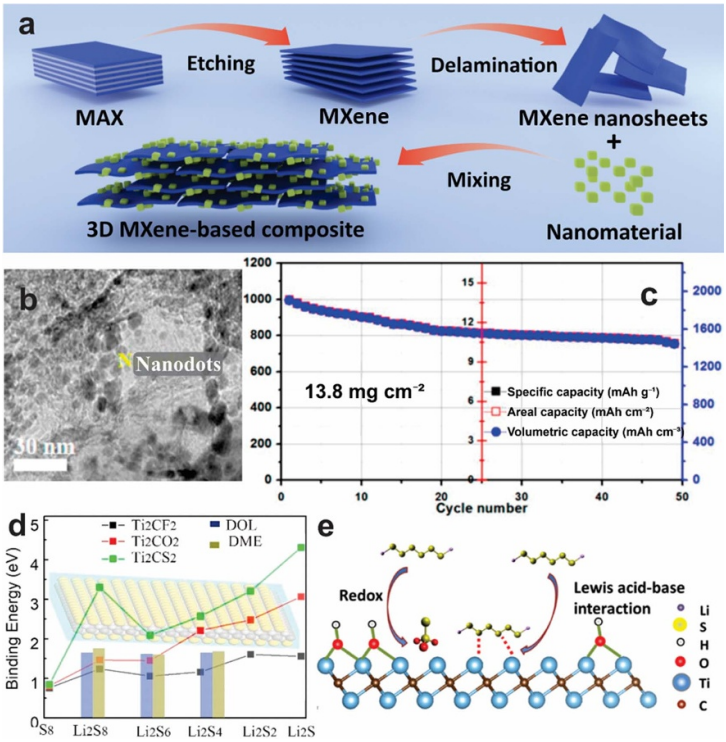

Figure 1. (a) Schematic illustration of the synthesis procedure of a 3D MXene-based composite. (b) TEM image of the $Ti_3C_2T_x$ nanodots-interspersed $Ti_3C_2T_x$ nanosheet (TCD-TCS) composite, and (c) cycling performance at 0.05 C of the resulting TCD-TCS/S cathode composite with a high sulfur loading of 13.8 mg cm^{-2}. Reprinted with permission from [101]. Copyright 2019, American Chemical Society. (d) Binding energies between sulfur redox intermediates and different MXene substrates: Ti_2CF_2, Ti_2CO_2 and Ti_2CS_2. Reprinted with permission from [102]. Copyright 2018, with permission from Elsevier. (e) Schematic illustration of the dual-mode interaction of polysulfides on OH-functionalized MXene surface. Reprinted with permission from [88]. Copyright 2016, John Wiley & Sons.

with different transition metal elements (M = Ti, Cr, V, Nb, Hf and Zr) revealed that a smaller lattice parameter leads to stronger polysulfide binding affinity originating from Li–O interactions [112]. This finding explains that the $Cr_3C_2O_2$ MXene features the highest binding strength among the other $M_3C_2O_2$ (M = Ti, V, Nb, Hf and Zr) structures. Theoretical studies on the adsorption capacity of $Ti_3C_2T_2$ MXenes (T = N, S, O, P, F, and Cl) to polysulfide intermediates and the catalytic effect for the Li_2S decomposition during the delitiation process also show that S and O terminations are the most suitable choices for a moderate adsorption strength of sulfur-related species [113]. This behavior is highly desired since the polysulfide shuttle can be suppressed without active material decomposition [46].

Although, there has been a success in the first-principle understanding of the chemical interaction between lithium (poly)sulfide species and the self-functionalized surface of MXenes. The modeling of the performance of a MXene-based electrode at electrochemical conditions still remains as a big challenge due to the surface complexity of MXenes and, to some extent, rely on the limited computational resources [104, 105]. Further advances in computations and the development of a more thorough theory which will include electrolyte/electrode interactions, charge carrier transfer on the interface and ion diffusivities. All of these parameters should be predictable at varying electrode potential in an ideal case. Access to such key factors will allow us to rationally design MXene materials with optimized electrochemical properties for Li–S batteries but also other energy storage systems.

2.3. From experiments to first-principles modeling

As discussed in the previous section, there is still a gap between experiments and computational predictions that are caused by the differences between complex experimental conditions and restricted theoretical conditions—partially hampered by limited computational resources. However, the theoretical calculation is a powerful tool to explain experimental observations and to provide new insights on the rational design of electrode materials, rather than finding materials by trial and error [115, 116].

The early studies on MXenes as sulfur host demonstrated that the Ti_2C-based MXenes could form Ti–S bonds with polysulfide intermediates via Lewis acid-base interactions [49]. However, by combining x-ray photoelectron spectroscopy and DFT calculations help to better understand the chemical interaction of polysulfides on Ti_3C_2 and Ti_3CN MXene surfaces. The results of this combined investigation demonstrated that hydroxyl terminations on the MXene surface assist in the conversion of polysulfides to thiosulfate and

polythionate intermediates subsequently before Ti–S bonds are formed (figure 1(e)) [88]. The finding of this dual-mode behavior provides new insights into the polysulfide confinement mechanism and allows to clarify experimental observations, such as suppressed polysulfide shuttling, improved active material utilization and, consequently, boosted the electrochemical performance of MXene-comprised Li–S batteries. Similarly, the outstanding electrochemical performance of novel sulfur host substrates including lattice-doped MXenes like the nitrogen-doped Ti_3C_2 MXene [117], Co-based compounds [118], 2D MoN-VN heterostructures [119], VN/graphene [120] and MgB_2/graphene [121] composites have been explained by combining both experimental and theoretical approaches.

A comprehensive understanding of MXene properties and their relationships to absorb or chemically interact otherwise with the sulfur species, formed during reaction in a beneficial way, can only be achieved in tandem with advanced (in situ, operando) characterization techniques and computation. The resulting fundamental information will be crucial to establish reaction mechanisms and uncover their detailed steps and to provide directions for the rational design of optimized sulfur cathode materials to enable a highly stable and reliable battery chemistry to go forward to advanced Li–S batteries, e.g. to a minimized version with high-energy density, specific and volumetric.

3. After reaching a stable battery chemistry: miniaturization of sulfur electrodes for micro Li–S batteries

The recent social and technical progresses have led to large variety of sensors, actuators and microcomputing devices. Therefore, it has been just a question of time until these applications are brought to the market as miniaturized and ideally self-powered systems for human self-optimization or diverse technical monitoring approaches. Miniaturization of self-powered, portable and flexible technologies like implantable biosensors, microelectromechanical systems and wearable gadgets has raised an urgent need for high-performance and, likewise, miniaturized energy storage devices. Typical miniaturized energy storage systems include conventional Li-ion microbatteries and microsupercapacitors. However, their limited energy density restricts their use in advanced microdevices with increasing electric power consumption. Therefore, it is highly required to investigate alternative electrochemical energy storage systems beyond Li-ion microbatteries and microsupercapacitors to satisfy the requirements of forthcoming micro- and nano-systems [122]. After enabling a stable battery chemistry with the help of tailored MXenes and the rational design approach, the typical size of the battery may comprise different cell casings from scientific formats like Swagelok or coin cells up to cyclindric, e.g. 18650, and prismatic or even up to paper sheet-sized pouch cells, as the latter three formats are widely used for industrial productions. Reliably working Li–S batteries with such formats may provide a good (knowledge) basis to allow for the development of microbatteries. Miniaturizing the electrodes is dedicated for an application in wearable or smallest scale power sources that should also be provided for integrated microdevices. Typical different dimensionalities of the electrode architecture like fibers (1D), stacked/interdigitated (2D) configurations or as scaffolds and swiss-roll-like (3D) forms promise individually customizable solutions for a broad application. These solutions can range from wearable textile-integrated electronics for micro-characterization and -sensing up to telemetry devices [123–127]. To realize high performance properties like long cycle life or high capacities, optimized battery configurations for electrodes, electrolytes and current collectors must be established. Therefore, a large variety of processing technologies have been applied to fabricate miniaturized batteries. 1D electrodes were classically prepared by the pyrolyzation of polymeric fibers [128, 129] or thin-film deposition techniques like atomic layer [130], chemical vapor [123, 131, 132] and electro-deposition [133–136] or sputtering [137, 138]. With ultrathin and highly directed laser beams and the modification of semiconductor production equipment, lithography [139–141] and laser preparation [142–146] both become important for battery minimization. Besides all physical and chemical methods, the mechanical preparation by printing has evolved to a highly promising possibility to conceptualize microelectrodes and print complete batteries for the mass market where pastes and inks typically represent liquid techniques [147–152], laser-printing administers the material from coated filaments or ribbons to the desired substrate [143, 153]. By printing, all dimensions can be realized even up to multi-coaxial cable structures [152]. The variability of ink-based printing with MXenes was recently reviewed even beyond the energy storage horizon [154]. To enable a microbattery with a high performance, a design should be selected which mainly benefits from the highest amount of active materials. Here, one important measure is found in the amount of inactive material related to current collectors, separators or substrates that needs to be minimized. Along with the other microelectrode and microbattery designs, the 3D architecture seems to be preferred. It is characterized by a large surface area that supports an increased contact with the electrolyte and provides significantly more surface sites for Li^+ ion diffusion compared to the lower dimensional designs (figure 2). A better performance and energy density is therefore possible. On

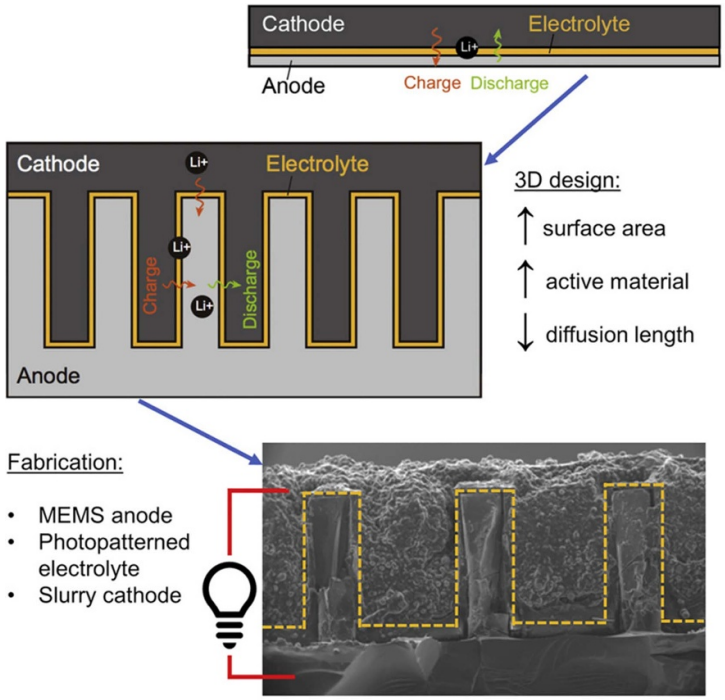

Figure 2. Schematic illustration of the advantages of a 3D microbattery vs a 2D thin-film microbattery. Reprinted with permission from [140]. Copyright 2018, with permission from Elsevier.

the other hand, producing fully 3D designs can technically be much more ambitious, especially on the nanoscale [155, 156].

Introducing MXenes into microstorage devices significantly increases the storage properties, namely areal and volumetric capacity or long-time stability, due to their highly tunable chemistry, packaging density and metallic conductivity [4, 9, 47]. First and most micro storage investigations have been described for supercapacitors [8, 157, 158] and preparations without additives were successfully realized [159, 160]. After deeply investigating the possibilities of MXenes for electrochemical microsupercapacitors, the MXene-based electrode concept has been introduced in Li-ion batteries with advancements in shortened ion diffusion length, higher in-plane charge carrier transport ability or chemically active storage sites [45, 161, 162]. The beneficial implementation of a MXene-based electrode in Li-ion microbatteries can be extracted from reported works as these examples show the potential of minimized MXene-based electrodes. Due to the preparation process, the final active material is not a MXene but anatase [163]. In another report the resulting thin-layer electrode is in the centimeter-scale for width and length of the electrode film [164].

Minimization of sulfur batteries will mainly follow printing or mechanical routes as sulfur in microelectronic fabrication equipment can cause undesirable effects like poisoning the whole system. Mechanically, a positive electrode for a Li–S microbattery was produced by twisting a CNT fiber after immersion in a suspension of *N,N*-dimethylformamide and sulfur, previously melt-infiltrated into the hierarchical carbon CMK-3 and coated with graphene oxide. The resulting positive fiber electrode was combined with a negative Li wire electrode inside a small plastic hose to give a cable-shaped Li–S (micro) battery. Here, the micrometer dimension is found in the diameter of the hose while the length is given in several centimeters. Nevertheless, this cable-shaped battery is able to power light-emitting diodes (LEDs) integrated in textiles even during stretching or bending of the fabric for at least 30 min depending on the number of electrode cables forming the battery and number of lighted LEDs [165]. Handling sulfur or sulfur-carbon composites by printing is an easy way to avoid negative impacts and enable diverse electrode layouts. For Li–S microbatteries, ink-based printing has successfully applied for sulfur positive electrodes [166, 167]. At the starting point, electrodes were printed from an aqueous ink containing aligned multiwall CNTs and dissolved polysulfides. For this first experiment, a dispenser was used while the electrodes were filtered-off on a nylon membrane masked with glass tubes of about 3 mm in inner diameter [166]. To advance this first simple setup, the same group developed an ink-based printing process where single-wall CNTs with infused sulfur were suspended in cyclohexylpyrrolidone. With the help of an inkjet printer drops of 10 pL were reached and electrodes with 2 × 2 mm and 5 × 5 mm were printed on different substrates. During galvanostatic cycling both electrodes completed 100 full cycles without large capacity fade starting at about 790 mAh g^{-1} and 850 mAh g^{-1}, respectively, at 0.5 C. In the 100th cycle the 2 × 2 mm electrode still

delivered about 650 mAh g^{-1} and the 5 × 5 mm electrode about 790 mAh g^{-1} [167]. Besides the solvent-assisted printing a dry laser-based process was described. To produce the laser-printed sulfur positive electrodes, the laser-induced forward transfer was applied. To finally print the electrode, a layered material stack was designed which consisted of a glass-donor substrate coated with a triazene polymer acting as the lifting agent and the carbon-binder composite. For sulfur, a second donor substrate was prepared. By irradiation with an UV-laser the triazene layer decomposes and carries the material to the target. With this process several layers of carbon-binder and sulfur were laminated onto the target. Here, the ablated sulfur deeply infiltrated the carbon layer. Assembled versus a lithium metal anode in a micro pouch cell, the Li–S microbattery delivered 1200 mAh g^{-1} in the initial cycle. After 400 cycles, about 950 mAh g^{-1} were still obtained at a C-rate of 1. At 2 C and 3 C this microbattery just slightly decreased in the performance over 400 cycles. At a C-rate >3, discharging drops to significantly lower specific capacities [168].

To miniaturize a positive sulfur electrode for a thin-film battery application, a layer-by-layer assembly method was reported. The resulting electrodes were used for charging and discharging tests in CR2032 coin cells but no microbattery application has been described [169]. Nevertheless, this kind of assembly could be within the realms of possibility in the future.

MXenes have been used for the preparation of sulfur positive electrodes as it has emerged to positively act as a good chemically active host scaffold. These materials offer an almost metallically conducting network to contact the individual sulfur particles. It results in fast charge carrier transport properties with a relatively low effort. Additionally, the mechanical stability of MXenes also shows a sufficient strength to withstand the volume expansion according to Li_2S formation during the lithiation of sulfur [47]. One first related approach was found in the etching of the Ti_2SC MAX phase. After the exfoliation of the C/S-nanolaminates, the resulting positive electrode worked properly [170]. Besides the direct preparation of an electrode composite from a MAX phase, Ti_2AlC was first chosen to prepare MXene/sulfur composites. Therefore, Al was etched away from the respective layers and sulfur was melt-infiltrated. For long-term cycling, 700 cycles were reported with an initial specific capacity of about 1100 mAh g^{-1} and about 800 mAh g^{-1} at the 700th cycle at 0.5 C [49]. Similar results were reported for the MXene $Ti_3C_2T_x$ prepared from Ti_3AlC_2 [171, 172]. These two publications underline the possibility to fabricate stable Li–S batteries with an extended lifetime compared to typical conductive carbon/sulfur composites and are easier to prepare compared to other porous carbon scaffolds. Additionally, high absorption properties for polysulfide species have been attributed to the MXene as the positive electrode composite main additive. Recently, researchers showed high and reversible absorption rates for sulfur species, like polysulfides and elemental sulfur with a loading of up to 76.5%, on highly porous carbon spheres combined with a MXene . The good performance is expressed by high Coulombic efficiencies of about 93% (in the first few cycles) and above 99% for all cycles beyond number five at 0.2 C and 1 C, respectively [173]. For more examples, the interested reader is referred to a review about applications of engineered MXene composites where much more additional information can be found going beyond the topic of this perspective [174].

As sulfur and Li_2S are isolating materials and need a very good conducting network to enable a satisfactory operation of a Li–S battery. MXenes with their metallic conductivity and tunable chemistry offer great opportunity to contribute as conductive and sulfur retarding additive. These properties directly support an increase in performance and can also function for sulfur batteries with high loadings. For this reason, MXenes will significantly impact the minimization of Li–S batteries. For Li–S microbattery electrodes prepared by printing as a less extensive method, MXenes can significantly influence the success of a minimization, especially when inkjet techniques are utilized.

4. Towards highly reliable Li–S (micro)batteries: self-healing composites for positive sulfur/MXene-containing electrodes

Additionally to an improved conductivity and charge carrier transport within the electrode composite, significantly supported by MXenes, the mechanical instability due to the volume changes of the different sulfur reaction states needs to be buffered. As multiple charging and discharging cycles, storage conditions and other phenomena stress the device-utilized materials, self-healing properties, at least for a single part of the cell, seem to be highly beneficial. Otherwise, the realization of a high-performance Li–S microbattery may become tricky in most cases. Inspired by the healing of skin wounds or bone fractures, self-healing is often reported for polymers and polymer-composites as well as for metals and alloys [175–178]. In the following the general mechanisms of self-healing polymers is shortly described for a better overview, as this class of materials is in the focus of this section.

For self-healing polymers, two main mechanisms are distinguished: (a) extrinsic and (b) intrinsic self-healing. For extrinsic self-healing, capsules or vascular networks with the healing agent, e.g. a polymerizable monomer, and a catalyst are deposited in the polymer matrix. For the capsule-based

self-healing four main scenarios are described. In the first the capsule contains the healing agent while the catalyst is dispersed in the polymer matrix. Additionally, functional groups of the polymer matrix phase can also catalyze the polymerization as a second possibility, called latent functionality. In a third example, both, healing agent and catalyst, are utilized in separate capsules (multicapsule system). For the fourth capsule-based scheme the catalyst is hosted in the capsule and the healing agent is phase-separated within the polymer matrix material or vice versa. A similar concept is found in vascular self-healing materials where the healing agent(s) are stored in hollow fibers [54, 55].

The intrinsic self-healing is a less complex concept compared to the extrensic one as the polymer matrix itself is used for the self-healing process. Five principle concepts are described where two are directly related to reversible bond formations. Here, bonds are connected via reactions, like retro-Diels–Alder and Diels–Alder reactions or via an ionomeric copolymer cluster that enables a reversible cross-linking. For supramolecular self-healing, strong end- or side-groups can associate with hydrogen-terminated groups to form reversible hydrogen bonds. Molecular diffusion is another option for a polymer to provide self-healing properties. In this case the self-healing ability is significantly correlated with time and temperature and typically progresses via void closure, surface interaction and molecular entanglement. A last possibility is the phase-separated disperison of a thermoplastic polymer as an additive in the polymer matrix [54, 55].

After a damage, a stimulus like elevated temperature or light induces the self-healing process in an ideal surrounding. The transfer of the self-healing concept into different applications including batteries may exert influences far beyond the desired conditions.

For ion batteries many examples exist, where polymers can help to repair the electrode active material, e.g. silicon microparticles of the negative electrode [179, 180]. Other solutions, which meet the self-healing aspect, comprise other cell parts. One solution is found in electrolyte additives. New electrolyte formulations with polysulfides enable a self-healing of the sulfur cathode [181]. For the Li–S battery, an improvement of storage performance is reached if a lithium metal anode is used. Due to side reactions and especially dendrite growth, the self-healing functionality was introduced by MPF_6-electrolyte additives (M = Cs, Rb, Ag). These compounds act as self-healing initiators according to an electrostatic shield mechanism (figure 3). The formation of metal dendrites is inhibited due to the support and the homogeneous re-deposition of lithium on the metal surface [182]. The concept to suppress dendrites on the Li metal anode was successfully applied for Li–S batteries with a composite of a sulfur-containing allyl polymer and inorganic sulfides. This composite forms during the contact with Li metal during electrochemical plating and stripping of lithium in a self-assembling reaction. During cycling, damaged parts of this artificial solid electrolyte interphase can self-heal what was attributed to the plasticizing property of the sulfur-allyl polymer in combination with the inorganic components [183].

All of the previously exemplified measures are dedicated to avoid sulfur depletion of the cathode or dendrite growth on the lithium metal anode. Their effects are often related to additional electrolyte additives that seem to work properly at the described, elaborated conditions. Nevertheless, these possibilities may also cause severe issues e.g. on the long-term scale or in industrial cells up to a possible malfunction, especially if electrolytes and their complicated chemistries in combination with more complex electrode architectures are considered. One important example is related to the addition of $LiNO_3$ to the Li–S battery electrolyte. Here, the lower voltage of the cyclable voltage window increases to 1.8 V. At lower voltages $LiNO_3$ participates in several reactions and is irreversibly consumed which is followed by lower lifetime and performance of the battery [184, 185]. On the other hand, the storable energy content is reduced due to the smaller voltage window. MXenes can sufficiently help to by-pass the need to utilize further electrolyte additives when combined e.g. with graphene. These composites sufficiently suppress the dendrite growth on the metal anode and show enhanced cycle life for Li–S batteries. Together with graphene, the $Ti_3C_2T_x$–MXene, functionalized with lithiophilic surface groups, acts as a host for metallic Li and enables a homogeneous re-deposition of Li during the plating process [186].

The positive aspect of self-healing of the sulfur cathode is found in some already existing solutions . Depending on the set-up of the Li–S cell, two application types of self-healing polymers can generally be considered, (a) as a polysulfide shuttle suppressing interlayer attached to the separator and (b) used as a binder in the electrode composite.

As a self-healing polymer interlayer concurrently acting as polysulfide barrier polydimethylsiloxane (PDMS)-based silly putty crosslinked by a transient B–O dynamic bond was suggested by Chang *et al* [187]. As a second example poly(dimethylsiloxane)–4,4′-ethylenebis(phenylisocyanate)–1,1′-thiocarbonyl-diimidazole (PDMS-MPI-TM) was proposed by Xu et al [188]. The self-healing process is promoted by thiourea moieties which were incorpatored into a microphase-separated polyurea network. These moieties suppress a crystallisation and enable reversible hydrogen bond cleavage and re-formation.

By saving the positive electrode and applying a modified separator an almost similar effect was reached with a MXene-containing solution. Via a self-assembling strategy with polyethyleneimine (PEI) and CNTs,

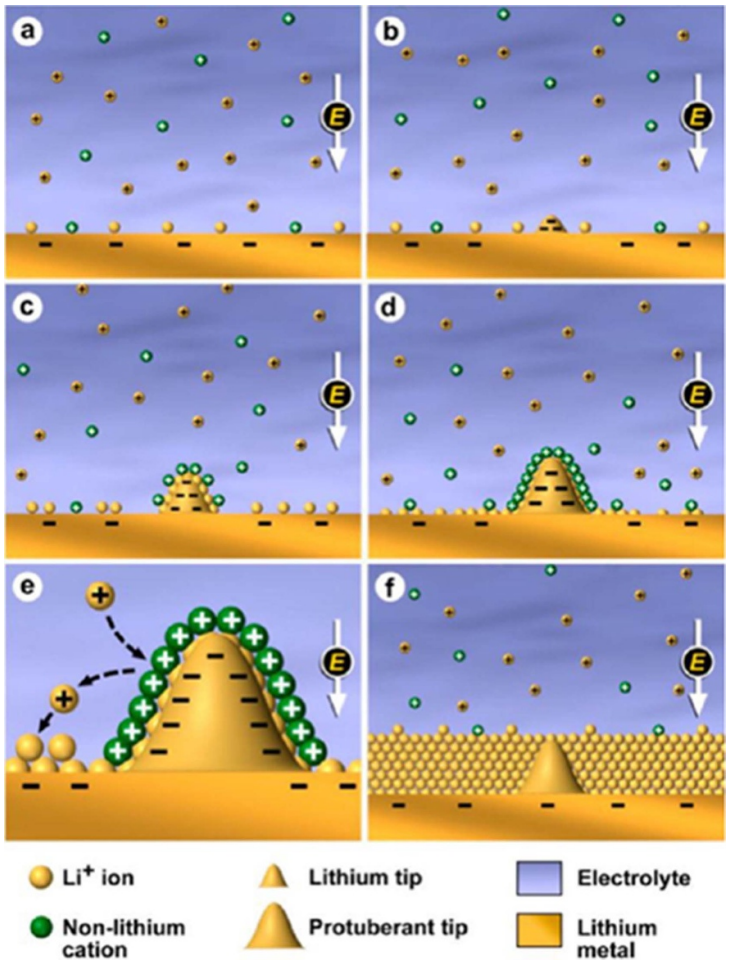

Figure 3. Illustration of Li deposition process based on the self-healing electrostatic shielding mechanism (a) initial deposition process of Li^+ and M^+ ion (M = Rb, Cs, Ag) on the lithium surface; (b) formation of protuberant tips due to system fluctuations at potentials slightly lower than Li^+ ion reduction but higher than M^+ ion reduction; (c) lower overpotential on the tips initiate dendrite growth, first electrostatic sorption of M^+ ions; (d) accumulation of M^+ ions in the vicinity of the tip to form an electrostatic shield; (e) positively charged shield repels Li^+ ion forcing Li deposition at adjacent regions; (f) smooth Li metal deposition. Reprinted with permission from [182]. Copyright 2013, American Chemical Society.

the $Ti_3C_2T_x$-MXene was implemented into a basic conductive 3D network where about 5.8 mg_S cm^{-2} was infiltrated. A low amount of electrolyte of partially only 12 ml $g^{-1}{}_S$ was utilized. Afterwards, the MXene-CNT-PEI mixture was coated onto usual glass fiber separator. Both, the optimized cathode and the functionalized separator well-improved the overall cell performance up to 1100 mAh g^{-1} at 0.5 C for 200 cycles at the minimum [189]. For composites with PEI, CNTs and cellulose nanocrystals or a latex rubber [190] and with branched PEI and epoxy resins [191] or branched PEI with graphite [192], self-healing was already described. This effect may appear in the MXene-CNT-PEI composite as well but was not reported [189].

Aside from the strategy to provide self-healing interlayers, developing self-healing binders for the sulfur-containing cathode composite can be considered as a serious and perhaps favored alternative. A supramolecular polymer consisting of poly(*N*-ethyl-*N*'-hexyl-1,4,5,8-naphthalenetetracarboxydiimidyl methacrylate-co-triethyleneglycol methyl ether methacrylate)(PENDI) with naphtalene diimide side chains crosslinked to triPy linkers containing pyrene units was published by Qin et al [193]. This kind of polymers showed robust self-healing properties and was applied in Li–S cells. In their review, Xu et al [54] proposed polyurethane- and polyurea-based polymers with several flexible side chains like PDMS to allow for an introduction as self-healing binders in Li–S batteries. Even metallic centers like Fe or Co in a carboxylic coordination can support self-healing and polysulfide capture in hierarchically organized polymers.

Building not only a better but a highly reliable sulfur cathode with self-healing components, used as interlayer or binder (see a performance check in table S1, available online at stacks.iop.org/JPENERGY/3/021002/mmedia), are possible and may open an interesting field of investigation as it can significantly help to improve reversible cycling and therewith prolongs the lifetime of the device and lowers serious negatively impacting side reactions. Even with additives like MXenes, electrodes with

self-healing properties can be realized. Nevertheless, taking the advantage of self-healing electrodes into account, it will have to be discussed in detail, if this possibility can be applied to the whole cell and all electrodes or just to individual parts. Additionally, specific options for certain battery operation scenarios with application of self-healing polymers will help to come to the necessary conclusion of how this topic may positively influence Li–S battery performance, also in a microstorage application. As a recommendation, one of the concepts should be realized to establish such highly reliable, minimized Li–S batteries, preferably the binder. Both concepts implemented in one cell may be contradictory for real production. To implement both, the interlayer and the binder, into the cell at least one more production step must be installed to the line resulting in higher costs.

5. Coupling energy (micro)harvesting and Li–S energy microstorage systems: the way to autonomous power sources

To continue the minimization philosophy of batteries and to go beyond, it can be helpful to couple these microstorage devices with the respective power sources to avoid complex transformation procedures e.g. to make use of the line current. The results of this combination is an autonomous power source dedicated to field applications in wearable electronics but also e.g. in seismic sensors or in other sensor and actuator systems which may be out of reach for a regular maintenance or power source exchange.

Coupling an energy storage device and an electrical power generator, mainly via the power grid, is a traditional method to enable recharging. What is well established at the macroscopic scale, e.g. pumped hydro storage and a megawatt-power plant, may be similarly established at the microscale. Bringing both systems together on the microscale to make the battery self-charging, large efforts have been made reaching a broad variety of solutions within the last 20 years and are still swiftly on-going. After the description of the minimization strategies for batteries, similar techniques have been applied for the development of microscopic power generators. Here, it is highly beneficial to take advantage of the desired harvesting functionality that can be combined easier or in a more complex construction with the storage device. However, it is also very helpful to motivate such a development with the dedicated operation site and what kind of energy can be converted to electric power. Many power generator concepts have been realized at the microscale. Most prominent examples are solar cells [194–199], triboelectric [197, 198, 200, 201] and piezoelectric [197, 198, 201–203] or, nowadays, thermoelectric generators [198, 204–207]. Along with these well-studied nanogenerators, novel techniques have been developed where one or even more concepts of energy harvesting are combined like in fuel cell-derived systems, e.g. microbial [208], photocatalytic [209] and enzymatic fuel cells [210] or based on physical concepts like thermomagnetic devices [211]. Coupling of the aforementioned systems is also described on the microscale for a thermoelectric element with a fuel cell [212] or a vibrational device [213].

As battery and power generator are widely established on the microscale, the crucial step is their wedding (borrowed from car manufacturing). This concept means combining both units in one compartment to fulfill their individual function as energy storage and energy harvesting devices, but acting as one autonomous power unit that enables stable electrical power supply which can be operated completely independent of an external plug. As indicated above, one prominent example are medical implants. Here, these devices should not be explanted or should not need a cable connection to just charge the battery, e.g. placed in a pacemaker. It is noted that in principle all wearable electronics without emphasis on the body-interior or -exterior can make use of the self-charging of the energy storage device by a nanogenerator.

The recently most appropriate storage system to be combined with a harvester has been found with supercapacitors. The supercapacitors were often selected as these devices can be fabricated by similar techniques like the harvesting system itself, e.g. semiconductor industry-derived processes. Additionally, it benefits of less complicated chemistry, as in principle just a relatively large specific surface area is needed. A further advantage is found in the broad developments reported on high specific surface materials. At least both the harvesting and the storage device can make use of the same electrolyte. Therefore, combinations of the diverse nanoscopic power generators with supercapacitors of 1D- and 2D-architectures have been realized for solar energy harvesting [214–216]. Another large and highly investigated field is the conversion and utilization of human motion energy [217]. Human motion energy is often harvested by triboelectric or piezoelectric devices [217–223]. Coupling the harvester with an energy storage, again supercapacitors [224–228] or Li-ion capacitors [229] are widely spread due to the same advantages as mentioned above. Additionally, batteries have been reported, as e.g. fiber-shaped Li-ion batteries woven to a fabric or flexible designs and are established as such storage systems [230–232]. Similar utilization and coupling are found for thermoelectric power generators which have been combined with a supercapacitor [233] and a solid-state battery [234] whereas for the diverse fuel cell-derived power generators supercapacitors seem to be preferred as well, when talking about integrated devices [208–210]. Combinations of nanogenerators with different

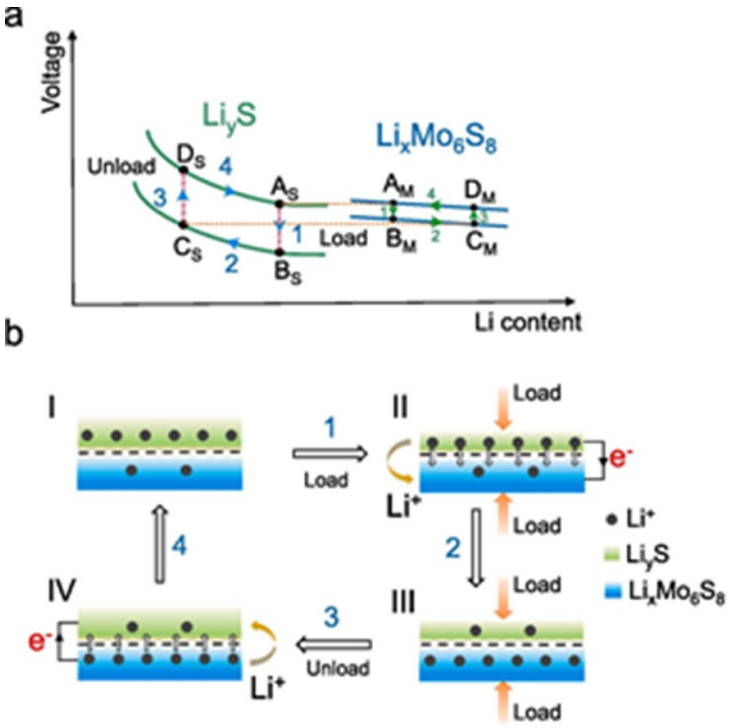

Figure 4. Working principle of the ICEC device. (a) Four thermodynamic states of the electrodes during a compression-decompression cycle. (b) A schematic view of the compression-decompression cycle. The four states are: (I) An isopotential state in the two electrodes is attained by short-circuiting via an external wire. (II) Compression on ICEC device induces chemical potential difference of Li between the electrodes, driving Li^+ and e^- migration from Li_yS to $Li_xMo_6S_8$. (III) A new isopotential equilibrium is reached. (IV) Upon removing the compressive stress, Li^+ and e^- flow back, and the original state I is recovered. Reprinted with from [240]. Copyright 2020, with permission from Elsevier.

physical energy conversion principles coupled to an energy storage device have additionally been reported [235–237].

To route back to the sulfur-battery related application of nanoscopic power generators and to make use of the three to five times higher specific capacity compared to classical Li-ion batteries, one interesting concept was realized for a Li–S battery with a liquid alkaline polysulfide cathode. Here, the cathode is recharged by a Pt/CdS photocatalyst that leads to a targeted oxidation of reduced/discharged ionic S^{2-} sulfur species. As a side reaction, hydrogen is produced. With a discharge capacity of 762 mAh g^{-1}, this type of battery can exceed other batteries of the Li-ion type [238]. Nevertheless, as a hydrogen producer, a consumer may be needed that can be realized with a fuel cell system. Therefore, this cell type can be of valuable interest in mobile devices or vehicles.

To harvest mechanical energy with Li–S cells, an interesting concept has been proposed which, in principle, coincides with a triboelectric nanoscopic power generator and a Li–S battery. Electrochemically lithiated $Li_xMo_6S_8$ and Li_yS act as an intercalation and a conversion electrode, respectively. Using a filter paper as the separator, a water-based lithium bis(trifluoro-methane sulfonyl)imide- and lithium triflate-containing electrolyte, that also serves as the hydraulic medium with respect to its incompressibility, complete the device called intercalation-conversion electrode couple (ICEC). The authors highlighted four advantages over classical triboelectric harvesters and Li–S batteries: (a) The entire harvester generates power under pressure. (b) A possible while easy scale-up of the active volume is due to the uniform pressure distribution with respect to the geometry. (c) A larger working area is expected compared to a pressure-asymmetric device. In the latter, the working area is only limited to the bending region. (d) The final advantage is the aqueous electrolyte (figure 4).

The working principle corresponds to a Carnot cycle [239]. First, an isopotential state is attained by externally short-circuiting both electrodes. In the second state, the device is compressed and the pressure load initiates the migration of Li^+ ions and electrons by a difference in the chemical potential of both electrodes. After the charge carrier migration has stopped, a new isopotential third state has been reached. In state four the compressive load is removed and both charge carriers re-equilibrate to the initial first state. The investigated ICEC device reached a current of 736 μA cm^{-2} which corresponds to a power output of 143 μW cm^{-2} [240]. It has to be noted, that the reported results are a proof-of-principle. Recently, a few research works have been reported in which MXenes were integrated into triboelectric nanogenerator devices

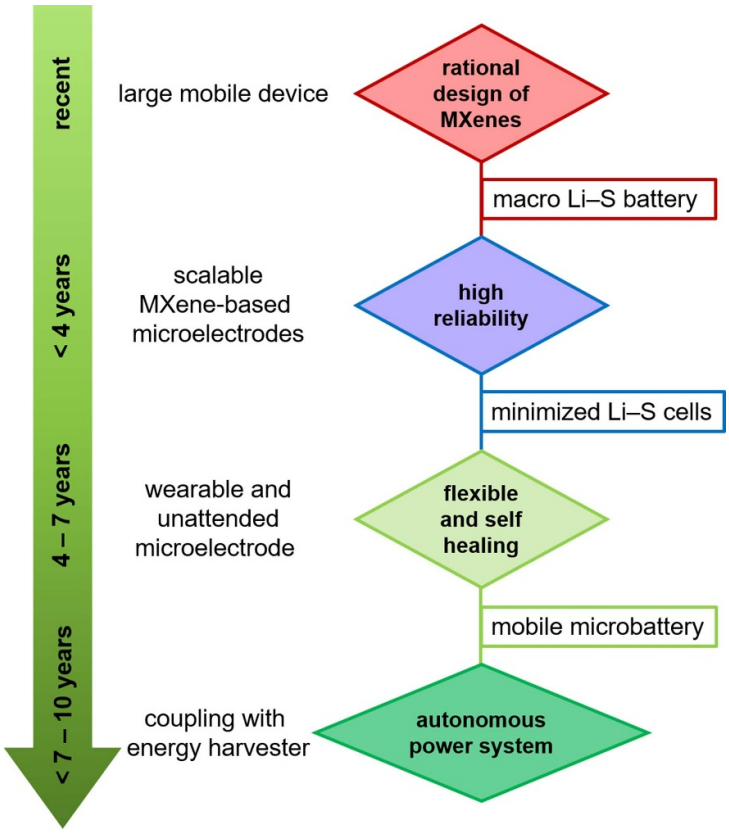

Figure 5. Flowchart to efficient autonomous power supply systems with the help of Li–S batteries and MXenes.

[241–243]. Alongside the advancements in MXene processing, further research in the direction of nanoscopic power generators and sulfur-based microbatteries will most probably be realized in the near future.

6. Future perspectives

To support the recent efforts, we suggest a possible development like presented in the flowchart scheme in figure 5. Here, some to our opinion necessary major milestones are identified. After solving the issues coupled to these milestones step-by-step, even cheap autonomous electrical energy supply systems with suitable performance come into a reachable range. As a first step, rational design may play a critical role as with this tool appropriate materials can be developed that solve or even by-pass at least some of the previously described issues. With this starting point reliable electrodes and therewith Li–S batteries will be prepared that enable a strategy to minimize the complete battery. With several techniques like inkjet printing, it seems to be feasible on a relatively short time scale. Along with the minimization process, other challenges will appear, e.g. low sulfur content on the cathode according to the high density of MXenes compared to carbons or the resulting conductivity problems for high sulfur loadings without any measures. A possible solution is found in the advanced engineering of MXenes to enable high sulfur loadings of up to 10.5 mg cm^{-2}. It is noted that other carbons are avoided with this preparation [244]. Multidimensional composites with delaminated MXenes as one main component can be used similarly [89, 174]. Even for these small cells electrode breathing can neither be excluded nor neglected and can significantly decrease the lifetime and reliability. Polymer additives with self-healing properties—the re-formation of chemical bonds in a polymer—can be treated as one important measure to enlarge the reliability of the electrode and therewith the whole cell. Within this aspect the self-discharging should be noted. Probably the self-healing polymers are able to stop a self-discharging via polysulfide shuttling in combination with the MXene. This possibility is exemplified by a polydopamine/MXene composite [100] but in the case presented here, the self-healing polymer and the MXene have to act similarly. With such well-designed tools it is not surprising that ambitious perspectives like autonomous micro power supplies with a combined harvesting and storage unit could be reached in the next 10 years. Although the time scales showed in figure 5 are conservatively estimated, faster development is possible depending on the advances in MXene materials and battery technology. Surely, the steps between the rational design of the materials until the autonomous electrical

energy supply can be vitally discussed as the order may not necessarily follow the paths as suggested in figure 5. Nevertheless, starting with rational design to come to an optimal material, in this case the MXenes for an application in Li–S batteries, definitely seems like a good start.

With the previously described possible achievements in the background, it sounds technically reasonable to establish a MXene-based system with a nanoscopic power generator and a Li–S cell where the harvesting unit is produced of a MXene-based composite and the electrodes of the sulfur cell as well. The literature presents many examples where both electrodes benefit from the employed MXene or a MXene composite. The unique properties of MXenes, as already mentioned before, like almost metallic electrical conductivity and the possibility to rationally design the surface groups, lattice and porosity or even the possibility to print microdevices with MXenes will pave the way to produce microscale self-charging Li–S batteries. Here, the way to successfully establish this technology may also lead via a quasi-solid-state battery with a gel-electrolyte and a polysulfide suppressing separator, probably with a MXene as well [245]. In another case, solid-state Li–S batteries as the upcoming technology can significantly contribute with the help of the previously suggested approaches [245, 246]. It is underlined here, that this possible scenario does not represent the final stage. Most probably, more iterations will be necessary to reach the presented milestones. We suppose that MXene materials for energy storage systems will continue the quick and interesting progress since some innovative works have already been realized. Many new aspects will be learned on the path from the rational design to the autonomous micro power system but, hopefully, some important findings can be introduced in the large devices or even other sulfur batteries as well.

Acknowledgments

JB acknowledges the Agencia Nacional de Promoción Científica y Tecnológica (FONCYT-PICT No. 2017-0824) and Ministerio de Ciencia y Tecnología (MINCyT-Córdoba, GRFT Res. 79/2018) for funding support.

LG is indebted to all who have supported many ideas, has helped to realize these and have had great cooperations.

ORCID iDs

Juan Balach https://orcid.org/0000-0002-7396-1449
Lars Giebeler https://orcid.org/0000-0002-6703-8447

References

[1] Novoselov K S, Geim A K, Morozov S V, Jaing D, Zhang Y, Dubonos S V, Grigorieva I V and Firsov A A 2004 *Science* **306** 666–9
[2] Geim A K and Novoselov K S 2007 *Nat. Mater.* **6** 183–91
[3] Naguib M, Kurtoglu M, Presser V, Lu J, Niu J, Heon M, Hultman L, Gogotsi Y and Barsoum M W 2011 *Adv. Mater.* **23** 4248–53
[4] Gogotsi Y and Anisori B 2019 *ACS Nano* **13** 8491–4
[5] Khazaei M, Ranjbar A, Arai M, Sasaki T and Yunoki S 2017 *J. Mater. Chem.* C **5** 2488–503
[6] Verger L, Xu C, Natu V, Cheng H-M, Ren W and Barsoum M W 2019 *Curr. Opin. Solid State Mater. Sci.* **23** 149–63
[7] Persson P O Å and Rosen J 2019 *Curr. Opin. Solid State Mater. Sci.* **23** 100774
[8] Eklund P, Rosen J and Persson P O Å 2017 *J. Phys. D: Appl. Phys.* **50** 113001
[9] Verger L, Natu V, Carey M and Barsoum M W 2019 *Trends Chem.* **1** 656–69
[10] Anasori B and Gogotsi Y 2019 *2D Metal Carbides and Nitrides (Mxenes), Structure, Properties and Applications* (Berlin: Springer)
[11] Pang J, Mendes R G, Bachmatiuk A, Zhao L, Ta H Q, Gemming T, Liu H, Liu Z and Rümmeli M H 2019 *Chem. Soc. Rev.* **48** 72–133
[12] Khazaei M, Mishra A, Venkataramanan N S, Singh A K and Yunoki S 2019 *Curr. Opin. Solid State Mater. Sci.* **23** 164–78
[13] Ling Z, Ren C E, Zhao M-Q, Yang J, Giammarco J M, Qiu J, Barsoum M W and Gogotsi Y 2014 *Proc. Natl Acad. Sci.* **111** 16676–81
[14] Venkateshala S and Grace A N 2020 *Appl. Mater. Today* **18** 100509
[15] Fang R *et al* 2020 *ChemSusChem* **13** 1409–19
[16] Das P and Wu Z-S 2020 *J. Phys. Energy* **2** 032004
[17] Garg R, Agarwal A and Agarwal M 2020 *Mater. Res. Express* **7** 022001
[18] Sun S, Liao C, Hafez A M, Zhu H and Wu S 2018 *Chem. Eng. J.* **338** 27–45
[19] Jimmy J and Kandasubramanian B 2020 *Eur. Polym. J.* **122** 109367
[20] Wang Y, Xu Y, Hu M, Ling H and Zhu X 2020 *Nanophotonics* **9** 1601–20
[21] Xin M, Li J, Ma Z, Pan L and Shi Y 2020 *Front. Chem.* **8** 297
[22] Kim H, Wang Z and Alshareef H N 2019 *Nano Energy* **60** 179–97
[23] Kim H and Alshareef H N 2020 *ACS Mater. Lett.* **2** 55–70
[24] Hantanasirisakul K and Gogotsi Y 2018 *Adv. Mater.* **30** 1804779
[25] Shahzad F, Alhabeb M, Hatter C B, Anasori B, Hong S M, Koo C M and Gogotsi Y 2016 *Science* **353** 1137–40
[26] Iqbal A, Sambyal P and Koo C M 2020 *Adv. Funct. Mater.* **30** 2000883
[27] Guo Z, Miao N, Zhou J, Sa B and Sun Z 2017 *J. Mater. Chem.* C **5** 978–84
[28] Wu L *et al* 2018 *Laser Photonics Rev.* **12** 1800215
[29] Jhon Y I, Koo J, Anasori B, Seo M, Lee J H, Gogotsi Y and Jhon Y M 2017 *Adv. Mater.* **29** 1702496
[30] Wu Q, Wang Y, Huang W, Wang C, Zheng Z, Zhang M and Zhang H 2020 *Photonics Res.* **8** 1140–7

[31] Feng T, Li X, Guo P, Zhang Y, Liu J and Zhang H 2020 *Nanophotonics* **9** 2505–13
[32] Montazeri K, Currie M, Verger L, Dianat P, Barsoum M W and Nabet B 2019 *Adv. Mater.* **31** 1903271
[33] Yi J *et al* 2019 *2D Mater.* **6** 045038
[34] Soleymaniha M, Shahbazi M-A, Rafieerad A R, Maleki A and Amiri A 2019 *Adv. Healthcare Mater.* **8** 1801137
[35] Meng F *et al* 2018 *ACS Nano* **12** 10518–28
[36] Ward E J, Lacey J, Crua C, Dymond M K, Maleski K, Hantanasirisakul K, Gogotsi Y and Sandeman S 2020 *Adv. Funct. Mater.* **30** 2000841
[37] Shamsabadi A A, Ghahfarokhi M S, Anasori B and Soroush M 2018 *ACS Sustain. Chem. Eng.* **6** 16586–96
[38] Srimuk P, Halim J, Lee J, Tao Q, Rosen J and Presser V 2018 *ACS Sustain. Chem. Eng.* **6** 3739–47
[39] Ihsanullah I 2020 *Nano-Micro Lett.* **12** 72
[40] Rasool K, Pandey R P, Rasheed P A, Buczek S, Gogotsi Y and Mahmoud K A 2019 *Mater. Today* **30** 80–102
[41] Xue Q *et al* 2017 *Adv. Mater.* **29** 1604847
[42] Mei J, Ayoko G A, Hu C, Bell J M and Sun Z 2020 *Sustain. Mater. Technol.* **25** e00156
[43] Ng V M H, Huang H, Zhou K, Lee P S, Que W, Xu J Z and Kong L B 2017 *J. Mater. Chem.* A **5** 3039–68
[44] Anasori B, Lukatskaya M R and Gogotsi Y 2017 *Nat. Rev. Mater.* **2** 16098
[45] Zhang X, Zhang Z and Zhou Z 2018 *J. Energy Chem.* **27** 73–85
[46] Balach J, Linnemann J, Jaumann T and Giebeler L 2018 *J. Mater. Chem.* A **6** 23127–68
[47] Zhang C J, Ma Y, Zhang X, Abdolhosseinzadeh S, Sheng H, Lan W, Pakdel A, Heier J and Nüesch F 2020 *Energy Environ. Mater.* **3** 29–55
[48] Tontini G, Greaves M, Ghosh S, Bayram V and Barg S 2020 *J. Phys. Mater.* **3** 022001
[49] Liang X, Garsuch A and Nazar L F 2015 *Angew. Chem., Int. Ed. Engl.* **54** 3907–11
[50] Zhou L, Danilov D L, Eichel R-A and Notten P H L 2020 *Adv. Energy Mater.* 2001304
[51] Jin Q, Li L, Wang H, Gao H, Zhu C and Zhang X 2019 *Electrochim. Acta* **312** 149–56
[52] Tang H *et al* 2018 *Adv. Sci.* **5** 1800502
[53] Pomerantseva E, Bonaccorso F, Feng X, Cui Y and Gogotsi Y 2019 *Science* **366** eaan8285
[54] Xu J, Ding C, Chen P, Tan L, Chen C and Fu J 2020 *Appl. Phys. Rev.* **7** 031304
[55] Blaiszik B J, Kramer S L B, Olugebefola S C, Moore J S, Sottos N R and White S R 2010 *Annu. Rev. Mater. Res.* **40** 179–211
[56] Huttunen K M, Raunio H and Rautio J 2011 *Pharmacol. Rev.* **63** 750–711
[57] Naderi M, Lemoine J M, Govindaraj R G, Kana O Z, Feinstein W P and Brylinski M 2019 *Brief. Bioinform.* **20** 2167–84
[58] Bramwell V W and Perrie Y 2005 *Drug Discov. Today* **10** 1527–34
[59] Annabi N, Tamayol A, Uqillas J A, Akbari M, Bertassoni L E, Cha C, Camci-Unal G, Dokmeci M R, Peppas N A and Khademhosseini A 2014 *Adv. Mater.* **26** 85–124
[60] Allcock H R 1992 *Science* **255** 1106–12
[61] Balke B, Wurmehl S, Fecher G H, Felser C and Kübler J 2008 *Sci. Technol. Adv. Mater.* **9** 014102
[62] Akhmetshina T G, Blatov V A, Proserpio D M and Shevchenko A P 2018 *Acc. Chem. Res.* **51** 21–30
[63] Dos Santos L H R 2020 *J. Mol. Struct.* **1203** 127431
[64] Tranchemontagne D J, Ni Z, O´Keeffe M and Yaghi O M 2008 *Angew. Chem., Int. Ed. Engl.* **47** 5136–47
[65] Farha O K and Hupp J T 2010 *Acc. Chem. Res.* **43** 1166–75
[66] El-Kaderi H M, Hunt J R, Mendoza-Cortés J L, Côté A P, Taylor R E, O´Keeffe M and Yaghi O M 2007 *Science* **316** 268–72
[67] Kirschhock C E A, Kremer S P B, Vermant J, Van Tendeloo G, Jacobs P A and Martens J A 2005 *Chem. Eur. J.* **11** 4306–13
[68] Cantin A, Corma A, Diaz-Cabanas M J, Jordá J L and Moliner M 2006 *J. Am. Chem. Soc.* **128** 4216–7
[69] Serre C, Taulelle F and Ferey G 2003 *Chem. Commun.* **2003** 2755–65
[70] Casalnuevo A L, Calabrese J C and Milstein D 1988 *J. Am. Chem. Soc.* **110** 6738–44
[71] Shimidzu K D, Snapper M L and Hoveyda A H 1998 *Chem. Eur. J.* **4** 1885–9
[72] Baiker A 2000 *J. Mol. Catal.* A **163** 205–20
[73] Schlögl R 1998 *Angew. Chem., Int. Ed. Engl.* **37** 2333–6
[74] Tang Y, Zhang Y, Li W, Ma B and Chen X 2015 *Chem. Soc. Rev.* **44** 5926–40
[75] Yuan R, Kang W and Zhang C 2018 *Materials* **11** 937
[76] Cui L, Zhou L, Kang Y-M and An Q 2020 *ChemSusChem* **13** 1071–92
[77] Yao X, Zhao Y, Castro F A and Mai L 2019 *ACS Energy Lett.* **4** 771–8
[78] Wu X-L, Guo Y-G and Wan L-J 2013 *Chem. Asian J.* **8** 1948–58
[79] Jana M, Xu R, Cheng X-B, Yeon J S, Park J M, Zhang Q and Park H S 2020 *Energy Environ. Sci.* **13** 1049–75
[80] Xu H, Long Q and Manthiram A 2016 *Nano Energy* **26** 224–32
[81] Zhai S, Wei L, Karahan H E, Chen X, Wang C, Zhang X, Chen J, Wang X and Chen Y 2019 *Energy Storage Mater.* **19** 102–23
[82] Tang X, Guo X, Wu W and Wang G 2018 *Adv. Energy Mater.* **8** 1801897
[83] Zhang C J, Cui L, Abdolhosseinzadeh S and Heier J 2020 *InfoMat* **2** 613–38
[84] Balach J, Jaumann T, Mühlenhoff S, Eckert J and Giebeler L 2016 *Chem. Commun.* **52** 8134–7
[85] Zhang Z-W, Peng H-J, Zhao M and Huang J-Q 2018 *Adv. Funct. Mater.* **28** 1707536
[86] Maletti S, Podetti F S, Oswald S, Giebeler L, Barbero C A, Mikhailova D and Balach J 2020 *ACS Appl. Energy Mater.* **3** 2893–9
[87] Hong X, Wang R, Liu Y, Fu J, Liang J and Dou S 2020 *J. Energy Chem.* **42** 144–68
[88] Liang X, Rangom Y, Kwok C Y, Pang Q and Nazar L F 2016 *Adv. Mater.* **29** 1603040
[89] Bao W, Xie X, Xu J, Guo X, Song J, Wu W, Su D and Wang G 2017 *Chem. Eur. J.* **23** 12613–9
[90] Wang Z, Zhang N, Yu M, Liu J, Wang S and Qiu J 2019 *J. Energy Chem.* **37** 183–91
[91] Song J, Guo X, Zhang J, Chen Y, Zhang C, Luo L, Wang F and Wang G 2019 *J. Mater. Chem.* A **7** 6507–13
[92] Wang J, Zhang Z, Yan X, Zhang S, Wu Z, Zhuang Z and Han W-Q 2020 *Nano-Micro Lett.* **12** 4
[93] Lv L-P, Guo C-F, Sun W and Wang Y 2019 *Small* **15** 1804338
[94] Zhou H-Y, Sui Z-Y, Amin K, Lin L-W, Wang H-Y and Han B-H 2020 *ACS Appl. Mater. Interfaces* **12** 13904–13
[95] Bao W, Liu L, Wang C, Choi S, Wang D and Wang G 2018 *Adv. Energy Mater.* **8** 1702485
[96] Zhang H, Qi Q, Zhang P, Zheng W, Chen J, Zhou A, Tian W, Zhang W and Sun Z M 2019 *ACS Appl. Energy Mater.* **2** 705–14
[97] Pan H, Huang X, Zhang R, Wang D, Chen Y, Duan X and Wen G 2019 *Chem. Eng. J.* **358** 1253–61
[98] Liu H, Zhang X, Zhu Y, Cao B, Zhu Q, Zhang P, Xu B, Wu F and Chen R 2019 *Nano-Micro Lett.* **11** 65
[99] Zhang Y *et al* 2018 *Adv. Funct. Mater.* **28** 1707578
[100] Wang X, Yang C, Xiong X, Chen G, Huang M, Wang J-H, Liu Y, Liu M and Huang K 2019 *Energy Storage Mater.* **16** 344–53

[101] Xiao Z, Li Z, Li P, Meng X and Wang R 2019 *ACS Nano* **13** 3609–17
[102] Liu X, Shao X, Li F and Zhao M 2018 *Appl. Surf. Sci.* **455** 522–6
[103] Hu T, Hu M, Gao B, Li W and Wang X 2018 *J. Phys. Chem.* C **122** 18501–9
[104] Fan Y, Chen X, Legut D and Zhang Q 2019 *Energy Storage Mater.* **16** 169–93
[105] Zhan C, Sun W, Xie Y, Jiang D-E and Kent P R C 2019 *ACS Appl. Mater. Interfaces* **11** 24885–905
[106] Sim E S, Yi G S, Je M, Lee Y and Chung Y-C 2017 *J. Power Sources* **342** 64–69
[107] Rao D, Zhang L, Wang Y, Meng Z, Qian X, Liu J, Shen X, Qiao G and Lu R 2017 *J. Phys. Chem.* C **121** 11047–54
[108] Zhao Y and Zhao J 2017 *Appl. Surf. Sci.* **412** 591–8
[109] Sim E S and Chung Y-C 2018 *Appl. Surf. Sci.* **435** 210–5
[110] Liang P, Zhang L, Wang D, Man X, Shu H, Wang L, Wan H, Du X and Wang H 2019 *Appl. Surf. Sci.* **489** 677–83
[111] Lin H, Yang -D-D, Lou N, Zhu S-G and Li H-Z 2019 *Ceram. Int.* **45** 1588–94
[112] Li N, Meng Q, Zhu X, Li Z, Ma J, Huang C, Song J and Fan J 2019 *Nanoscale* **11** 8485–93
[113] Wang D, Li F, Lian R, Xu J, Kan D, Liu Y, Chen G, Gogotsi Y and Wei Y 2019 *ACS Nano* **13** 11078–86
[114] Wang Y, Shen J, Xu L-C, Yang Z, Li R, Liu R and Li X 2019 *Phys. Chem. Chem. Phys.* **21** 18559–68
[115] Chen X, Hou T, Persson K A and Zhang Q 2019 *Mater. Today* **22** 142–58
[116] Ye C, Chao D, Shan J, Li H, Davey K and Qiao S-Z 2020 *Matter* **2** 323–44
[117] Jiang G, Zheng N, Chen X, Ding G, Li Y, Snu F and Li Y 2019 *Chem. Eng. J.* **373** 1309–18
[118] Zhou J *et al* 2018 *Joule* **2** 2681–93
[119] Ye C, Jiao Y, Jin H, Slattery A D, Davey K, Wang H and Qiao S-Z 2018 *Angew. Chem., Int. Ed. Engl.* **57** 16703–7
[120] Sun Z, Zhang J, Yin L, Hu G, Fang R, Cheng H-M and Li F 2017 *Nat. Commun.* **8** 14627
[121] Pang Q, Kwok C Y, Kundu D, Liang X and Nazar L F 2019 *Joule* **3** 136–48
[122] Zhu Z, Kan R, Hu S, He L, Hong X, Tang H and Luo W 2020 *Small* **16** 2003251
[123] Oudenhoven J F M, Baggetto L and Notten P H L 2011 *Adv. Energy Mater.* **1** 10–33
[124] Qu Z, Zhu M, Tang H, Liu L, Li Y and Schmidt O G 2020 *Energy Storage Mater.* **29** 17–41
[125] Jiang K and Weng Q 2020 *ChemSusChem* **13** 1420–46
[126] Nishizawa M and Uchida I 1999 *Electrochemistry* **67** 420–6
[127] Chen H *et al* 2014 *Sci. Rep.* **4** 3790
[128] Verbrugge M W and Koch B J 1996 *J. Electrochem. Soc.* **143** 24–31
[129] Maitra T, Sharma S, Srivastava A, Cho Y-K, Madou M and Sharma A 2012 *Carbon* **50** 1753–61
[130] Zhao Z, Kong Y, Zhang Z, Huang G and Mei Y 2020 *J. Mater. Res.* **35** 701–19
[131] Ren J, Li L, Chen C, Chen X, Cai Z, Qiu L, Wang Y, Zhu X and Peng H 2013 *Adv. Mater.* **25** 1155–9
[132] Ellis B L, Knauth P and Djenizian T 2014 *Adv. Mater.* **26** 3368–97
[133] Yufit V, Nathan M, Golodnitsky D and Peled E 2003 *J. Power Sources* **122** 169–73
[134] Edström K, Brandell D, Gustafson T and Nyholm L 2011 *Electrochem. Soc. Interface* **20** 41–46
[135] Pikul J H, Zang H G, Cho J, Braun P V and King W P 2013 *Nat. Commun.* **4** 1732
[136] Shaijumon M M, Perre E, Daffos B, Taberna P-L, Tarascon J-M and Simon P 2010 *Adv. Mater.* **22** 4978–81
[137] Bates J B, Dudney N J, Neudecker B, Ueda A and Evans C D 2000 *Solid State Ion.* **135** 33–45
[138] Sugiawati V A, Vacandio F, Perrin-Pellegrino C, Galeyeva A, Kurbatov A P and Djenizien T 2019 *Sci. Rep.* **9** 11172
[139] Kinoshita K, Song X, Kim J and Inaba M 1999 *J. Power Sources* **81–82** 170–5
[140] Hur J I, Smith L C and Dunn B 2018 *Joule* **2** 1187–201
[141] Ning H, Pikul J H, Zhang R, Li X, Xu S, Wang J, Rogers J A, King W P and Braun P V 2015 *Proc. Natl Acad. Sci.* **112** 6573–8
[142] Pfleging W 2018 *Nanophotonics* **7** 549–73
[143] Piqué A, Arnold C B, Kim H, Ollinger M and Sutto T E 2004 *Appl. Phys.* A **79** 783–6
[144] Julian C M and Mauger A 2019 *Coatings* **9** 389
[145] Duduta M, de Rivaz S, Clarke D R and Wood R J 2018 *Batter. Supercaps* **1** 131–4
[146] Wartena R, Curtright A E, Arnold C B, Piqué A and Swider-Lyons K E 2004 *J. Power Sources* **126** 193–202
[147] Sun K, Wei T-S, Ahn B Y, Seo J Y, Dillon S J and Lewis J A 2013 *Adv. Mater.* **25** 4539–43
[148] Farahani R D, Dubé M and Therriault D 2016 *Adv. Mater.* **28** 5794–821
[149] Choi K-H, Ahn D B and Lee S-Y 2018 *ACS Energy Lett.* **3** 220–36
[150] Chang P, Mei H, Zhou H, Dassios K G and Cheng L 2019 *J. Mater. Chem.* A **7** 4230–58
[151] Lee K-H, Ahn D B, Kim J-H, Lee J-W and Lee S-Y 2020 *Matter* **2** 345–59
[152] Ragones H, Vinegrad A, Ardel G, Goor M, Kamir Y, Dorfman M M, Gladkikh A and Golodnitsky D 2020 *J. Electrochem. Soc.* **167** 070503
[153] Pröll J, Kim H, Piqué A, Seifert H J and Pfleging W 2014 *J. Power Sources* **255** 116–24
[154] Zhang Y-Z, Wang Y, Jaing Q, El-Demellawi J K, Kim H and Alshareef H N 2020 *Adv. Mater.* **32** 1908486
[155] Nasreldin M, de Mulatier S, Delattre R, Ramuz M and Djenizian T 2020 *Adv. Mater. Technol.* **5** 2000412
[156] Beidaghi M and Wang C 2010 *Proc. SPIE* **7679** 76791G
[157] Peng -Y-Y, Akzum B, Kurra N, Zhao M-Q, Alhabeb M, Anasori B, Caglan Kumbur E, Alshareef H N, Ger M-D and Gogotsi Y 2016 *Energy Environ. Sci.* **9** 2847–54
[158] Huang H *et al* 2020 *Nano Energy* **69** 104431
[159] Zhang C J *et al* 2019 *Nat. Commun.* **10** 1795
[160] Orangi J, Hamade F, Davis V A and Beidaghi M 2020 *ACS Nano* **14** 640–50
[161] Xiong D, Li X, Bai Z and Lu S 2018 *Small* **14** 1703419
[162] Greaves M, Barg S and Bissett M A 2020 *Batter. Supercaps* **3** 214–35
[163] Tesfaye A T, Mashtalir O, Naguib M, Barsoum M W, Gogotsi Y and Djenizian T 2016 *ACS Appl. Mater. Interfaces* **8** 16670–6
[164] Yun J *et al* 2019 *ACS Appl. Mater. Interfaces* **11** 47929–38
[165] Fang X, Weng W, Ren J and Peng H 2016 *Adv. Mater.* **28** 491–6
[166] Milroy C and Manthiram A 2016 *Chem. Commun.* **52** 4282–5
[167] Milroy C A, Jang S, Fujimori T, Dodabalapur A and Manthiram A 2017 *Small* **13** 1603786
[168] Rosenberg S and Hintennach A 2014 *Russ. J. Electrochem.* **50** 327–35
[169] Jin K, Zhou X and Liu Z 2015 *Nanomaterials* **5** 1481–92
[170] Zhao M-Q *et al* 2015 *Angew. Chem., Int. Ed. Engl.* **54** 4810–4
[171] Zhao Q, Zhu Q, Miao J, Zhang P and Xu B 2019 *Nanoscale* **11** 8442–8

[172] Zhang S, Zhong N, Zhou X, Zhang M, Huang X, Yang X, Meng R and Liang X 2020 *Nano-Micro Lett.* **12** 112
[173] Qi Q, Zhang H, Zhang P, Bao Z, Zheng W, Tian W, Zhang W, Zhou M and Sun Z M 2020 *2D Mater.* **7** 025049
[174] Xiao Z, Li Z, Meng X and Wang R 2019 *J. Mater. Chem.* A **7** 22730–43
[175] Mauldin T C and Kessler M R 2010 *Int. Mater. Rev.* **2010** 317–46
[176] Aïssa B, Therriault D, Hadda E and Jamroz W 2012 *Adv. Mater. Sci. Eng.* **2012** 854203
[177] Binder W H (ed) 2013 *Self-healing Polymers—from Principles to Applications* (Weinheim: Wiley-VCH)
[178] Khan A, Jawaid M, Raveendran S N and Asiri A M (eds) 2020 *Self-healing Composite Materials—From Design to Applications* (Cambridge: Woodhead Publishing/Elsevier)
[179] Wang C, Wu H, Chen Z, McDowell M T, Cui Y and Bao Z 2013 *Nat. Chem.* **5** 1042–8
[180] Wang H, Wang P, Feng Y, Liu J, Wang J, Hu M, Wie J and Huang Y 2019 *ChemElectroChem* **6** 1605–22
[181] Xu R, Belharouak I, J C M L, Zhang X, Bloom I and Bareño J 2013 *Adv. Energy Mater.* **3** 833–8
[182] Ding F *et al* 2013 *J. Am. Chem. Soc.* **135** 4450–6
[183] Li G, Gao Y, He X, Huang Q, Chen S, Kim S H and Wang D 2017 *Nat. Commun.* **8** 850
[184] Zhang S S 2012 *J. Electrochem. Soc.* **159** A920–A923
[185] Rosenman A, Elazari R, Salitra G, Markevich E, Aurbach D and Garsuch A 2015 *J. Electrochem. Soc.* **162** A470–A473
[186] Shi H, Zhang C J, Lu P, Dong Y, Wen P and Wu Z-H 2019 *ACS Nano* **13** 14308–18
[187] Chang Z, He Y, Deng H, Li X, Wu S, Qiao Y, Wang P and Zhou H 2018 *Adv. Funct. Mater.* **28** 1804777
[188] Xu J H, Chen P, Wu J W, Hu P, Fu Y S, Jiang W and Fu J J 2019 *Chem. Mater.* **31** 7951–61
[189] Guo D *et al* 2019 *Nano Energy* **61** 478–85
[190] Liu X, Lu C, Wu X and Zhang X 2017 *J. Mater. Chem.* A **5** 9824–32
[191] Rohini R and Bose S 2015 *Phys. Chem. Chem. Phys.* **17** 7907–13
[192] Wu T and Chen B 2016 *J. Mater. Chem.* C **4** 4150–4
[193] Qin J, Lin F, Hubble D, Wang Y, Li Y, Murphy I A, Jang S-H, Yang J and Jen A K-Y 2019 *J. Mater. Chem.* A **7** 6773–83
[194] Li Q, Liu Y, Guo S and Zhou H 2017 *Nano Today* **16** 46–60
[195] Gurung A and Qiao Q 2018 *Joule* **2** 1217–30
[196] Schmidt D, Hager M D and Schubert U S 2016 *Adv. Energy Mater.* **6** 1500369
[197] Sun H, Zhang Y, Zhang J, Sun X and Peng H 2017 *Nat. Rev. Mater.* **2** 17023
[198] Wei H, Cui D, Ma J, Chu L, Zhao X, Song H, Liu H, Wang N, Liu T and Guo Z 2017 *J. Mater. Chem.* A **5** 1873–94
[199] Lau D, Song N, Hall C, Jiang Y, Lim S, Perez-Wurfl I, Ouyang Z and Lennon A 2019 *Mater. Today Energy* **13** 22–44
[200] Ahmad A, Hassan I, El-Kady M F, Radhi A, Jeong C K, Selvaganapathy P R, Zu J, Ren S, Wang Q and Kaner R B 2019 *Adv. Sci.* **6** 1802230
[201] Pu X, Hu W and Wang Z L 2018 *Small* **14** 1702817
[202] Briscoe J and Dunn S 2015 *Nano Energy* **14** 15–29
[203] Hu D, Yao M, Fan Y, Ma C, Fan M and Liu M 2019 *Nano Energy* **55** 288–304
[204] Yan J, Liao X, Yan D and Chen Y 2018 *IEEE J. Microelectromech. Syst.* **27** 1–18
[205] He R, Schierning G and Nielsch K 2018 *Adv. Mater. Technol.* **3** 1700256
[206] Jaziri N, Boughamoura A, Müller J, Mezghani B, Tounsi F and Ismail M 2020 *Energy Rep.* **6** 264–87
[207] Leonov V 2013 *IEEE Sens. J.* **13** 2384–91
[208] Santoro C, Soavi F, Serov A, Arbizzani C and Atanassov P 2016 *Biosens. Bioelectron.* **78** 229–35
[209] Qiu M, Sun P, Cui G, Tong Y and Mai W 2019 *ACS Nano* **13** 8246–55
[210] Pankratov D, Blum Z, Suyatin D B, Popov V O and Shleev S 2014 *ChemElectroChem* **1** 343–6
[211] Waske A, Dzekan D, Sellschopp K, Berger D, Stork A, Nielsch K and Fähler S 2019 *Nat. Energy* **4** 68–74
[212] Federici J A, Norton D G, Brüggemann T, Voit K W, Wetzel E D and Vlachos D G 2006 *J. Power Sources* **161** 1469–78
[213] Sato N *et al* 2007 *Japan. J. Appl. Phys.* A **46** 6062–7
[214] Chien C-T, Hiralal P, Wang D-Y, Huang I-S, Chen C-C, Chen C-W and Amaratunga G A J 2015 *Small* **11** 2929–37
[215] Wang Z, Cheng J, Huang H and Wang B 2020 *Energy Storage Mater.* **24** 255–64
[216] Xu J, Chen Y and Dai L 2015 *Nat. Commun.* **6** 9103
[217] Riemer R and Shapiro A 2011 *J. Neuroeng. Rehabil.* **8** 22
[218] Invernizzi F, Dulio S, Patrine M, Guizzetti G and Mustarelli P 2016 *Chem. Soc. Rev.* **45** 5455–73
[219] Tien M-H and D´Souza K 2020 *Proc. R. Soc.* A **476** 20190491
[220] Huang L, Lin S, Xu Z, Zhou H, Duan J, Hu B and Zhou J 2020 *Adv. Mater.* **32** 1902034
[221] Wei S, Hu H and He S 2013 *Smart Mater. Struct.* **22** 105020
[222] Geisler M, Boisseau S, Perez M, Gasnier P, Willemin J, Ait-Ali I and Perraud S 2017 *Smart Mater. Struct.* **26** 035028
[223] Ali F, Raza W, Li X, Gul H and Kim K-H 2019 *Nano Energy* **57** 879–902
[224] Wang J, Li X, Zi Y, Wang S, Li Z, Zheng L, Yi F, Li S and Wang Z L 2015 *Adv. Mater.* **27** 4830–6
[225] Guo H, Yeh M-H, Lai Y-C, Zi Y, Wu C, Wen Z, Hu C and Wang Z L 2016 *ACS Nano* **10** 10580–8
[226] Yuan L, Xiao X, Ding T, Zhong J, Zhang X, Shen Y, Hu B, Huang Y, Zhou J and Wang Z L 2012 *Angew. Chem., Int. Ed. Engl.* **51** 4934–8
[227] Ramadoss A, Saravanakumar B, Lee S W, Kim Y-S, Kim S J and Wang Z L 2015 *ACS Nano* **9** 4337–45
[228] He Z, Gao B, Li T, Liao J, Liu B, Liu X, Wang C, Feng Z and Gu Z 2019 *ACS Sustain. Chem. Eng.* **7** 1745–52
[229] Liang X, Qi R, Zhao M, Zhang Z, Liu M, Pu X, Wang Z L and Lu X 2020 *Energy Storage Mater.* **24** 297–303
[230] Zhang C, Zhu J, Lin H and Huang W 2018 *Adv. Mater. Technol.* **3** 1700302
[231] Pu X, Li L, Song H, Du C, Zhao Z, Jiang C, Cao G, Hu W and Wang Z L 2015 *Adv. Mater.* **27** 2472–8
[232] Zhao K, Yang Y, Liu X and Wang Z L 2017 *Adv. Energy Mater.* **7** 1700103
[233] Deng F, Qiu H, Chen J, Wang L and Wang B 2017 *IEEE Trans. Ind. Electron.* **64** 1477–85
[234] Carmo J P, Ribeiro J F, Silva M F, Goncalves L M and Correira J H 2010 *J. Micromech. Microeng.* **20** 085033
[235] Rajendran V, Vinu Mohan A M, Jayaraman M and Nakagawa T 2019 *Nano Energy* **65** 104055
[236] Gambier P, Anton S R, Kong N, Erturk A and Inman D J 2012 *Meas. Sci. Technol.* **23** 015101
[237] Zhang S L, Jiang Q, Wu Z, Ding W, Zhang L, Alshareef H N and Wang Z L 2019 *Adv. Energy Mater.* **9** 1900152
[238] Li N, Wang Y, Tang D and Zhou H 2015 *Angew. Chem., Int. Ed. Engl.* **54** 9271–4
[239] Carnot S 1872 *Ann. Sci. De l´É.N.S. 2nd Series.* **1** 393–457
[240] Xue W, Chen T, Ren Z, Kim S Y, Chen Y, Zhang P, Zhang S and Li J 2020 *Appl. Energy* **273** 115230
[241] Wang D, Lin Y, Hu D, Jiang P and Huang X 2020 *Composites* A **130** 105754

[242] Xu S, Dall'Agnese Y, Wei G, Zhang C, Gogosti Y and Han W 2018 *Nano Energy* **50** 479–88
[243] Jiang Q, Wu C, Wang Z, Wang A C, He J-H, Wang Z L and Alshareef H N 2018 *Nano Energy* **45** 266–72
[244] Xiao Z, Yang Z, Li Z, Li P and Wang R 2019 *ACS Nano* **13** 3404–12
[245] Bing D *et al* 2020 *Mater. Today* **40** 114–31
[246] Pan Q, Zheng Y, Kota S, Huang W, Wang S, Qi H, Kim S, Tu Y, Barsoum M W and Li C Y 2019 *Nanoscale Adv.* **1** 395–402